Physics Letters B 672 (2009) 35–44

Contents lists available at ScienceDirect

Physics Letters B

www.elsevier.com/locate/physletb

Lowest order QED radiative corrections to five-fold differential cross section of hadron leptoproduction

I. Akushevich [a], A. Ilyichev [b,*], M. Osipenko [c,d]

[a] Duke University, Durham, USA
[b] National Scientific and Educational Center of Particle and High Energy Physics of the Belarusian State University, 220040 Minsk, Belarus
[c] Istituto Nazionale di Fisica Nucleare, Sezione di Genova, 16146 Genoa, Italy
[d] Skobeltsyn Institute of Nuclear Physics, 119992 Moscow, Russia

ARTICLE INFO

Article history:
Received 30 November 2007
Received in revised form 9 December 2008
Accepted 21 December 2008
Available online 31 December 2008
Editor: W. Haxton

PACS:
13.40.Ks
13.60.-r

Keywords:
Radiative corrections
Semi-inclusive deep inelastic scattering
Exclusive radiative tail

ABSTRACT

The contribution of exclusive radiative tail to the cross section of semi-inclusive hadron leptoproduction has been calculated exactly for the first time. Although the experience of inclusive data analyses suggests us that the contribution of radiative tail from the elastic peak is of particular importance, similar effects in the semi-inclusive process were only recently estimated in the peaking approximation. The explicit expressions for the lepton part of the lowest order QED contribution of exclusive radiative tail to the five-fold differential cross section are obtained and discussed. Numerical estimates, provided within Jefferson Lab kinematic conditions, demonstrate rather large effects of the exclusive radiative tail in the region at semi-inclusive threshold and for high energy of detected hadron.

1. Introduction

The semi-inclusive deep inelastic scattering of a lepton on the nucleon represents an important tool for studying strong interaction. The possibility of representing a semi-inclusive hadron leptoproduction (SIHL) cross section as a convolution of the virtual photon absorption by the quarks inside the nucleon and the subsequent quark hadronization allows one to investigate these mechanisms separately. The SIHL experiment provides not only complete information on the longitudinal parton momentum distributions available in inclusive deep inelastic scattering (DIS) experiments, but also an insight on the hadronization process and on parton orbital momenta.

It is well known that SIHL events are altered by the real photon emission from the lepton and hadron legs as well as by additional virtual particle contributions. Due to (i) the fact that most of the outgoing particles in SIHL remain undetected and (ii) the finite resolution of experimental equipment, not all events with the real photon emission can be removed experimentally. Moreover, the contribution of events with an additional exchange of virtual particles cannot be removed at all. As a result the measured SIHL cross section includes not only the lowest order contribution which is the process of interest (Fig. 1(a)), but also the higher order effects whose contribution has to be removed from the data. Since the latter cannot be extracted by experimental methods, the corresponding radiative corrections (RC) have to be calculated theoretically.

The primary step in the solution of the task on RC calculation in the lepton nucleon scattering assumes the calculation of the part of the total lowest order QED correction that includes real photon emission from lepton leg as well as the additional virtual photon between the initial and final leptons and the correction due to virtual photon self-energy. There are two basic reasons for why other types of RC, such as box-type contribution or real photon emission from hadrons, are less important. The first is that these corrections do not contain the leading order contribution which is proportional to the logarithm of the lepton mass, and therefore, their contribution is much smaller comparing to RC from lepton part. The second is that the calculation of these effects requires additional assumptions about hadron interaction, so it has additional pure theoretical uncertainties, which are hardly controlled.

* Corresponding author.
E-mail addresses: igor.akushevich@duke.edu (I. Akushevich), ily@hep.by (A. Ilyichev), osipenko@ge.infn.it (M. Osipenko).

0370-2693/$ – see front matter
doi:10.1016/j.physletb.2008.12.058

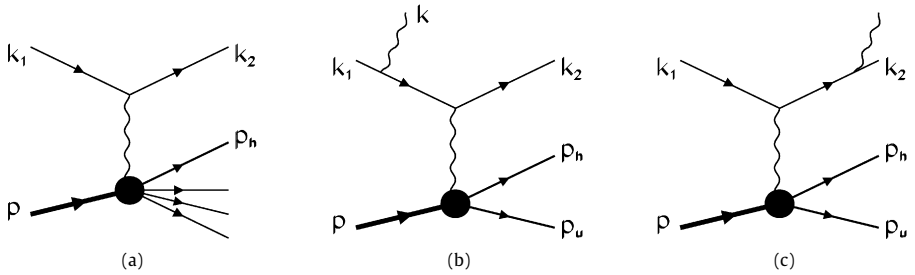

Fig. 1. Feynman graphs for the lowest order (a) and the exclusive radiative tail contributions to SIHL cross section with real photon emission from the initial (b) and final (c) leptons.

In the very first detailed SIHL experiments [1] RC were unknown and Monte Carlo simulations based on the approach from Ref. [2] were used to correct the data. The results of this Monte Carlo method however, have not been tested so far against the direct calculations of radiative effects. Meanwhile most experiments at high energies [3] neglected RC completely [4].

The calculations of the lepton part of the lowest order QED RC to SIHL cross sections were performed in Refs. [5,6] using Bardin–Shumeiko covariant approach [7]. In Ref. [5] the radiative effects were calculated for the three-dimensional cross section of unpolarized and polarized SIHL (target and lepton were longitudinally polarized) and the FORTRAN code for numerical estimates was provided as a patch (named SIRAD) to POLRAD code [8]. In Ref. [6] RC for the unpolarized five-fold differential cross section have been computed and FORTRAN code HAPRAD has been developed. However in both papers, RC do not include the contribution of the radiative tail from the exclusive reaction at the threshold. In inclusive DIS experiments analogous effects from the elastic radiative tail [2,9] give an important contribution to the observable cross section and, moreover, there exist kinematic regions (e.g. at high y or Q^2 and small x), where this contribution is dominant. This additional term of RC to SIHL has been investigated until now only in the peaking approximation [10].

In the present Letter the contribution of the lepton part of the lowest order QED RC to SIHL due to exclusive radiative tail is calculated exactly for the first time. This is done using the approach from Refs. [11,12] and notations from Ref. [6]. The RC were calculated for complete five-fold differential cross section. The technique of exact calculation of the lowest order RC (over α) is used in this Letter. The accuracy of the calculation is defined by accuracy of numerical integration, which can be easily controlled. Whereas actual values of the correction depend on the particular choice of the exclusive reaction parameters.

The rest of the Letter is organized as follows. In Section 2 we define kinematics of the investigated processes, obtain explicit expressions for the contribution of exclusive radiative tail to the five-fold differential cross section of SIHL, and investigate its analytical properties considering the soft photon limit. Discussion of the numerical results and concluding remarks are presented in Section 3. Also the explicit expressions allowing for the presentation of the results in closed form are given in Appendices A and B.

2. Kinematics and explicit expressions

Feynman graphs giving the Born as well as the lepton part of lowest order QED correction to SIHL cross section from the exclusive radiative tail are shown on Fig. 1(b), (c). The radiative tail is generated by the real photon emission from the lepton leg accompanying the exclusive leptoproduction:

$$l(k_1) + p(p) \to l'(k_2) + h(p_h) + u(p_u) + \gamma(k). \tag{1}$$

Following the notations of Ref. [6] we call measured in the final state hadron h, which is observed in coincidence with the scattered lepton l'. The second hadron u that completes the exclusive reaction remains undetected. Here k_1 (k_2) is the four-momentum of the initial (final) lepton ($k_1^2 = k_2^2 = m^2$), p is the target four-momentum ($p^2 = M^2$), p_h (p_u) is the four-momentum of the detected (undetected) hadron ($p_h^2 = m_h^2$, $p_u^2 = m_u^2$), and k is the emitted real photon four-momentum ($k^2 = 0$).

The set of variables describing the five-fold differential SIHL cross section can be chosen as follows:

$$x = -\frac{q^2}{2qp}, \quad y = \frac{qp}{k_1 p}, \quad z = \frac{p_h p}{pq}, \quad t = (q - p_h)^2, \quad \phi_h, \tag{2}$$

where $q = k_1 - k_2$ and ϕ_h is the angle between $(\mathbf{k}_1, \mathbf{k}_2)$ and $(\mathbf{q}, \mathbf{p}_h)$ planes in the target rest frame reference system ($\mathbf{p} = 0$).

For the description of the real photon emission we will use the following three variables:

$$R = 2kp, \quad \tau = \frac{2kq}{R}, \quad \phi_k \tag{3}$$

with ϕ_k being the angle between $(\mathbf{k}_1, \mathbf{k}_2)$ and $(\mathbf{q}, \mathbf{k})$ planes in the target rest frame reference system.

We also will use the following Lorentz invariants:

$$\begin{aligned}
&S = 2k_1 p, \qquad X = 2k_2 p = (1-y)S, \qquad Q^2 = -q^2 = xyS, \qquad W^2 = S_x - Q^2 + M^2, \qquad S_x = S - X,\\
&S_p = S + X, \qquad \lambda_q = S_x^2 + 4M^2 Q^2, \qquad \lambda_s = S^2 - 4M^2 m^2, \qquad V_{1,2} = 2k_{1,2} p_h = 2\big(a^{1,2} + b\cos\phi_h\big),\\
&\mu = \frac{2kp_h}{R} = 2\big(a^k + b^k \cos(\phi_k - \phi_h)\big), \qquad f = \frac{2k(p+q-p_h)}{R} = 1 + \tau - \mu,
\end{aligned} \tag{4}$$

where the explicit expressions for $a^{1,2,k}$, b and b^k coefficients can be found in Appendix B.

It is also useful to define the non-invariant quantities describing kinematics of the detected hadron such as its energy E_h, longitudinal p_l and transverse p_t three-momenta with respect to the virtual photon direction in the target rest frame. This quantities can be expressed through the Lorentz invariants introduced above in the following way:

$$E_h = z\nu = \frac{zS_x}{2M}, \qquad p_l = \frac{M}{\sqrt{\lambda_q}}\big(t - m_h^2 + Q^2 + 2\nu E_h\big), \qquad p_t^2 = E_h^2 - p_l^2 - m_h^2, \qquad \nu = \frac{S_x}{2M}, \tag{5}$$

where ν is a virtual photon energy in the targets rest frame.

Instead of the commonly accepted in SIHL analyses variable p_t^2 we will use the variable t. This is dictated not only by the fact that t is Lorentz invariant, but also by the necessity to distinguish the forward and backward hemispheres, mixed in the p_t^2-differential cross section. At intermediate energies of Jefferson Lab, the contribution of backward kinematics is significant, in particular for heavy hadrons detected in the final state. This backward kinematics is related to the target fragmentation mechanism described in terms of fracture functions [13]. Also one can notice that p_t^2-differential cross section is divergent in the completely transverse case $p_l = 0$ making difficult numerical integrations.[1]

According to Eq. (33) of Ref. [12] the contribution of the one-photon emission from the lepton leg to the exclusive hadron leptoproduction cross section can be presented as the integral of the squared matrix elements described by Fig. 1(b), (c) over the inelasticity $\nu = (p+q-p_h)^2 - m_u^2$ and the photon solid angle. The integration in our case is three-fold, because the measured exclusive cross section is four-dimensional and the cross section with emission of one additional photon is seven-dimensional. However, when we consider this contribution to the five-fold differential SIHL cross section, one photonic variable is fixed by measurement, and the contribution has a form of a two-dimensional integral. Specifically, we use the inelasticity ν as an observable in SIHL:

$$\nu = (1-z)S_x + t + M^2 - m_u^2. \tag{6}$$

At the same time the variable R is fixed by both observable and two photonic variables in the following way:

$$R = \frac{\nu}{f} = \frac{(1-z)S_x + t + M^2 - m_u^2}{1 + \tau - 2(a^k + b^k\cos(\phi_k - \phi_h))}. \tag{7}$$

Hence the integration over other two unobserved photonic variables: τ and ϕ_k requires for the calculation of the exclusive radiative tail contribution to SIHL.

The cross section responsible for the lepton part of the exclusive radiative tail (see Fig. 1(b), (c)) is given by

$$d\sigma_{\rm ex}^R = \frac{M_R^2}{2\sqrt{\lambda_s}(2\pi)^8}\frac{d^3k_2}{2E_2}\frac{d^3k}{2\omega}\frac{d^3p_h}{2E_h}\frac{d^3p_u}{2E_u}\delta^4(p+q-p_h-k-p_u) = \frac{M_R^2}{(4\pi)^7}\frac{RSS_x^2}{f\lambda_s\lambda_q}dx\,dy\,dz\,dt\,d\phi_h\,d\tau\,d\phi_k. \tag{8}$$

The squared matrix element M_R^2 can be presented as a convolution of the leptonic and hadronic tensors. The former has well-known structure:

$$L_{\mu\nu}^R = -\frac{1}{2}\,{\rm Tr}\big[(\hat{k}_2 + m)\Gamma_{\mu\alpha}(\hat{k}_1 + m)\hat{\Gamma}_{\alpha\nu}\big], \quad \Gamma_{\mu\alpha} = \left(\frac{k_{1\alpha}}{kk_1} - \frac{k_{2\alpha}}{kk_2}\right)\gamma_\mu - \frac{\gamma_\mu\hat{k}\gamma_\alpha}{2kk_1} - \frac{\gamma_\alpha\hat{k}\gamma_\mu}{2kk_2},$$
$$\hat{\Gamma}_{\alpha\nu} = \left(\frac{k_{1\alpha}}{kk_1} - \frac{k_{2\alpha}}{kk_2}\right)\gamma_\nu - \frac{\gamma_\alpha\hat{k}\gamma_\nu}{2kk_1} - \frac{\gamma_\nu\hat{k}\gamma_\alpha}{2kk_2}, \tag{9}$$

while the latter can be presented in a following covariant way:

$$W^{\mu\nu} = -\tilde{g}^{\mu\nu}\mathcal{H}_1 + \tilde{p}^\mu\tilde{p}^\nu\mathcal{H}_2 + \tilde{p}_h^\mu\tilde{p}_h^\nu\mathcal{H}_3 + (\tilde{p}^\mu\tilde{p}_h^\nu + \tilde{p}_h^\mu\tilde{p}^\nu)\mathcal{H}_4 \tag{10}$$

where

$$\tilde{g}^{\mu\nu} = g^{\mu\nu} + \frac{q^\mu q^\nu}{Q^2}, \qquad \tilde{p}^\mu = p^\mu + \frac{q^\mu pq}{Q^2}, \qquad \tilde{p}_h^\mu = p_h^\mu + \frac{q^\mu p_h q}{Q^2}, \tag{11}$$

and the Lorentz invariant structure functions $\mathcal{H}_i$ can be related to the exclusive photoabsorption cross sections as shown in Appendix A. After convolution of the leptonic and hadronic tensors the squared matrix element reads:

$$M_R^2 = \frac{(4\pi\alpha)^3}{\tilde{Q}^4}L_{\mu\nu}^R W_{\mu\nu} = -\frac{2(4\pi\alpha)^3}{\tilde{Q}^4 R}\sum_i \theta_i\mathcal{H}_i. \tag{12}$$

Combining Eqs. (8) and (12) we obtain the contribution of the exclusive radiative tail to SIHL cross section:

$$\frac{d\sigma_{\rm ex}^R}{dx\,dy\,dz\,dt\,d\phi_h} = -\frac{\alpha^3 SS_x^2}{2^7\pi^4\lambda_s\lambda_q}\int\limits_{\tau_{\rm min}}^{\tau_{\rm max}} d\tau\int\limits_0^{2\pi} d\phi_k\sum_{i=1}^4\theta_i(\tau,\phi_k)\frac{\mathcal{H}_i(\tilde{W}^2,\tilde{Q}^2,\tilde{t})}{f\tilde{Q}^4}. \tag{13}$$

The integration limits over τ are given by $\tau_{\rm min,max} = (S_x \pm \sqrt{\lambda_q})/2M^2$. Quantities $\theta_i(\tau,\phi_k)$ have the following form:

$$\theta_i(\tau,\phi_k) = \frac{4F_{IR}\theta_i^B}{R} + \theta_{i2} + R\theta_{i3}, \tag{14}$$

[1] See Fig. 3 and comments after Eq. (26) for details.

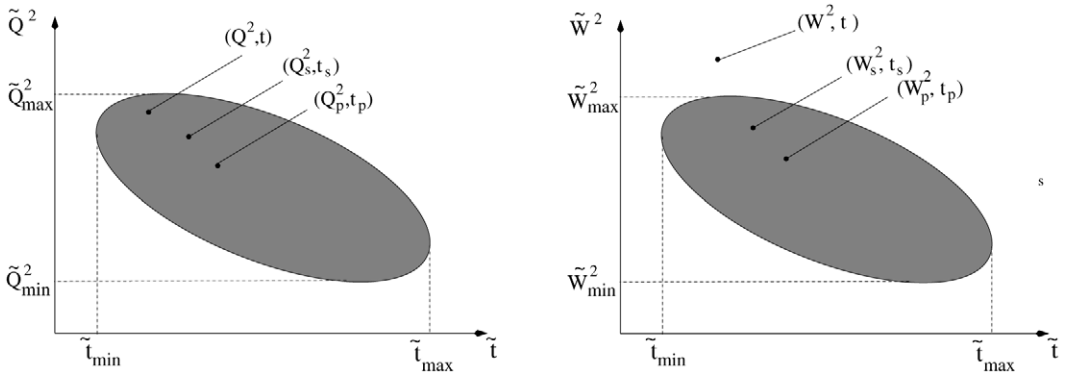

Fig. 2. The region of changes variables $\tilde{Q}^2$, $\tilde{W}^2$ and $\tilde{t}$: Born point is defined as (Q^2,t), (W^2,t). Two points corresponding to the collinear photon emission along initial and final leptons are presented as (Q_s^2,t_s), (W_s^2,t_s) and (Q_p^2,t_p), (W_p^2,t_p), respectively.

where F_{IR}, θ_{i2} and θ_{i3} are defined in Appendix B and

$$\theta_1^B = Q^2 - 2m^2, \qquad \theta_2^B = \big(SX - M^2Q^2\big)/2, \qquad \theta_3^B = \big(V_1V_2 - m_h^2Q^2\big)/2, \qquad \theta_4^B = \big(V_2S + V_1X - zQ^2S_x\big)/2. \tag{15}$$

The structure functions $\mathcal{H}_i$ depend on shifted kinematic variables modified with respect to ordinary ones by the real photon emission:

$$\tilde{W}^2 = (p+q-k)^2 = W^2 - R(1+\tau), \qquad \tilde{Q}^2 = -(q-k)^2 = Q^2 + R\tau, \qquad \tilde{t} = (q-p_h-k)^2 = t + R - v. \tag{16}$$

The region of changes for these variables is depicted in Fig. 2. Maximum and minimum values of these variables are defined in the following way:

$$\tilde{W}^2_{\max/\min} = W^2 - \frac{v(C_{W^2} \mp \sqrt{C_{W^2}^2 - 4W^2(v+m_u^2)})}{2(v+m_u^2)}, \qquad \tilde{Q}^2_{\max/\min} = Q^2 - \frac{v(C_{Q^2} \mp \sqrt{C_{Q^2}^2 + 4Q^2(v+m_u^2)})}{2(v+m_u^2)},$$
$$\tilde{t}_{\max/\min} = t - \frac{v(C_t \mp \sqrt{C_t^2 - 4t(v+m_u^2)})}{2(v+m_u^2)}, \tag{17}$$

where $C_{W^2} = W^2 + v - m_h^2 + m_u^2$, $C_{Q^2} = Q^2 - S_x - t + m_h^2$ and $C_t = t + v - M^2 + m_u^2$.

In this figure one can see the Born point as well as points that correspond to the so-called collinear singularity (that was only used in [10] for peaking approximation): $\tau = \tau_s \equiv -Q^2/S$ ($\tau = \tau_p \equiv Q^2/X$), $\phi_k = 0$, when the real photon is emitted along the momentum of the initial (final) lepton. These points correspond to the following shifted variables:

$$W_{s,p}^2 = W^2 - R_{s,p}(1+\tau_{s,p}), \qquad Q_{s,p}^2 = Q^2 + R_{s,p}\tau_{s,p}, \qquad t_{s,p} = t + R_{s,p} - v, \tag{18}$$

where

$$R_s = \frac{vS\lambda_q}{\lambda_q(S-Q^2) + (SS_x + 2Q^2M^2)t_q - zQ^2S_xS_p + 2\sqrt{\Lambda}\cos(\phi_h)p_t},$$
$$R_p = \frac{vX\lambda_q}{\lambda_q(X+Q^2) + (XS_x - 2Q^2M^2)t_q - zQ^2S_xS_p + 2\sqrt{\Lambda}\cos(\phi_h)p_t}, \tag{19}$$

$t_q = t + Q^2 - m_h^2$ and $\Lambda = Q^2\lambda_q(SX - M^2Q^2)$.

If in Eq. (13) we restrict our consideration only to the soft photon emission the result has to be proportional to the Born contribution to the exclusive cross section with a coefficient, independent of type of considered process. To obtain this well-known relation between contributions of the soft-photon emission and the Born to the cross section of the exclusive process, it is necessary to integrate Eq. (13) over z keeping only the photons with energy ω in the limits: $\omega_{\min} \leqslant \omega \leqslant \omega_{\max} \ll$ *all energies and masses*. The corresponding Born contribution reproduces the cross section of the exclusive leptoproduction and can be expressed in terms of the coefficients (15) and the structure functions $\mathcal{H}_i$:

$$\frac{d\sigma_{\rm ex}^B}{dx\,dy\,dt\,d\phi_h} = \frac{\alpha^2 SS_x}{16\pi^2 Q^4\lambda_s\sqrt{\lambda_q}} \sum_{i=1}^{4} \mathcal{H}_i\big(W^2, Q^2, t\big) \lim_{z\to z_0} \theta_i^B. \tag{20}$$

The integration variable z and the photon energy in the target rest frame are related as

$$z = \frac{t + S_x + M^2 - m_u^2 - 2fM\omega}{S_x}, \tag{21}$$

while the limit z_0 corresponds to the situation when emitted photon energy is equal to zero: $z_0 = (t + S_x + M^2 - m_u^2)/S_x$.

Therefore taking into account

$$\int_{\tau_{\min}}^{\tau_{\max}} d\tau \int_0^{2\pi} d\phi_k\, F_{IR} = -4\pi\sqrt{\lambda_q}\left(\frac{Q^2+2m^2}{\sqrt{\lambda_m}} \log\frac{\sqrt{\lambda_m}+Q^2}{\sqrt{\lambda_m}-Q^2} - 1\right), \tag{22}$$

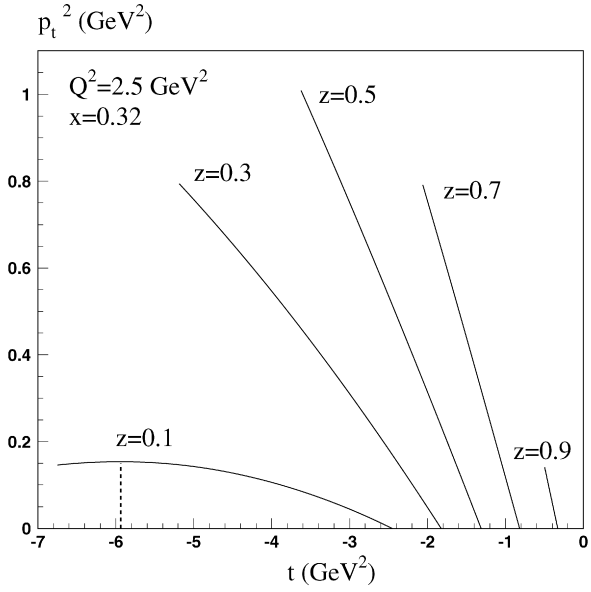

Fig. 3. t-dependence of p_t^2 at different z. The dashed line shows t-points where p_l changes sign.

where $\lambda_m = Q^2(Q^2+4m^2)$, finally we obtain the sought equality in the form:

$$\frac{d\sigma_{\rm ex}^{\rm soft}}{dx\,dy\,dt\,d\phi_h} = \frac{2\alpha}{\pi}\log\frac{\omega_{\max}}{\omega_{\min}}\left(\frac{Q^2+2m^2}{\sqrt{\lambda_m}}\log\frac{\sqrt{\lambda_m}+Q^2}{\sqrt{\lambda_m}-Q^2}-1\right)\frac{d\sigma_{\rm ex}^{B}}{dx\,dy\,dt\,d\phi_h}, \tag{23}$$

or, in the limit $m\to 0$,

$$\frac{d\sigma_{\rm ex}^{\rm soft}}{dx\,dy\,dt\,d\phi_h} = \frac{2\alpha}{\pi}\log\frac{\omega_{\max}}{\omega_{\min}}\left(\log\frac{Q^2}{m^2}-1\right)\frac{d\sigma_{\rm ex}^{B}}{dx\,dy\,dt\,d\phi_h}. \tag{24}$$

Thus, we reproduced expected result for the cross section of soft photon irradiation (e.g., see Eq. (7.64) of [14]).

3. Discussion of numerical results and concluding remarks

In this section the contribution of the exclusive radiative tail is illustrated in several examples investigated under kinematical conditions of the current experiments on the SIHL measurements. For this purpose the FORTRAN code was developed.[2]

Most recent experiments measuring SIHL are being performed at Jefferson Lab. In particular, the large acceptance of CLAS detector allows for extraction of the information about the five-fold differential SIHL cross section in a rather wide kinematic region that covers almost the whole z-range as well as the entire ϕ_h-range. In this section we present numerical results for the five-fold differential SIHL cross section in CLAS kinematic conditions.

One remark has to be discussed before presenting numerical estimates. Consider t-dependence of p_t^2 at fixed Q^2, x and different z that is presented in Fig. 3 for π^+-electroproduction in electron–proton scattering. The upper t-limit corresponds to the maximum value of the detected hadron longitudinal momentum p_l:

$$t_{\max} = m_h^2 - Q^2 + \frac{1}{2M^2}\left(\sqrt{\lambda_q\left(z^2S_x^2-4M^2m_h^2\right)}-zS_x^2\right), \tag{25}$$

while the lowest one at low energy is given by the SIHL threshold

$$t_{\min} = (m_u+m_\pi)^2 - M^2 - (1-z)S_x, \tag{26}$$

i.e. when missing mass square

$$M_X^2 = (p+q-p_h)^2 = (1-z)S_x + t + M^2 \tag{27}$$

reaches its minimal value. Here m_π is a pion mass. A remarkable feature of this plot is that the curve $z=0.1$ crosses the point where p_l changes the sign and both positive and negative values of p_l give the same p_t. As it was mentioned above, due to the common denominator $|p_l|$ the p_t^2-differential SIHL cross section diverges at this point.

To estimate the value of RC we introduce the radiative correction factor in the standard way

$$\delta = \frac{\sigma_{\rm obs}}{\sigma_B}, \tag{28}$$

where $\sigma_{\rm obs}$ (σ_B) is the radiatively corrected (Born) five-fold differential cross section of the semi-inclusive hadron leptoproduction.

[2] This code is available at http://www.hep.by/RC.

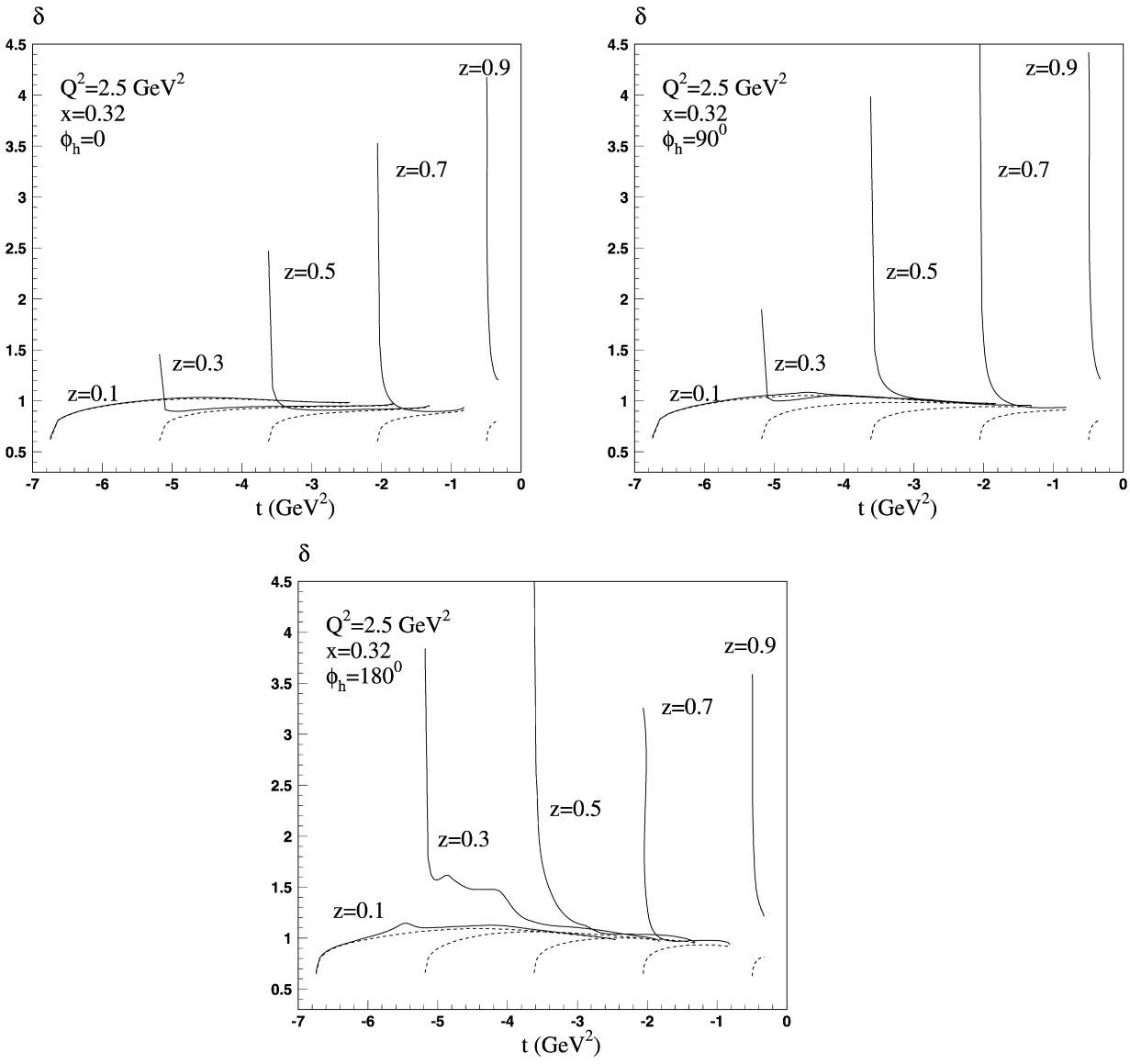

Fig. 4. t-dependence of the RC factor (28) for the semi-inclusive π^+ electroproduction at fixed proton for lepton beam energy 6 GeV: solid lines show the total correction, dashed lines represent the correction excluding the exclusive radiative tail calculated in this Letter.

The analytical expressions of RC obtained in previous section can be applied to leptoproduction of any hadrons observable in the lepton–nucleon scattering. However we restrict our numerical studies to the case of π^+ production in electron–proton scattering. The calculation of RC factor requires applying the parameterization of the photoabsorption cross sections. We use the model developed by collaboration MAID 2003 [15]. This model provides parameterizations for each of the required photoabsorption cross sections which are continuous in whole kinematic region. It accurately predicts the behavior of the photoabsorption cross sections in the resonance region and has true asymptotic behavior for higher W and Q^2 by means of the fit from Ref. [16]. The numerical estimation of this effect requires knowledge of the structure functions within the kinematical restriction for the shifted variables presented in Fig. 2. However the most important region is concentrated near the s- and p-collinear singularity (see Eq. (18)) where the integrand expression reaches its maximum value. A possible effect of the specific choice of photoabsorption cross sections (e.g., choice of the MAID 2003 model) can be investigated by comparing the predictions of the model with experimental data or other model predictions in this particular region. For example, the CLAS kinematics restrictions (i.e. $E_{\text{beam}} = 6$ GeV, 1 GeV$^2 < Q^2 < 7$ GeV^2, $0 < p_t < 1.5$ GeV) for collinear singularity region are 0.07 GeV$^2 < Q^2_{s,p} < 10$ GeV^2, 1.17 GeV$^2 < W^2_{s,p} < 10$ GeV^2 and -8 GeV$^2 < t_{s,p} < 8 \times 10^{-3}$ GeV^2. Since the MAID 2003 describes experimental data in this region sufficiently well [15] (at least for $d\sigma_L/d\Omega_h$ and $d\sigma_T/d\Omega_h$ provided the main contribution for the total cross section) and provides convenient parametric form for all required photoproduction cross sections, the choice of the MAID 2003 seems to be reasonable and practical. In application of data analyses collected in the specific regions especially in situations when the other two photoabsorption cross sections $d\sigma_{TT}/d\Omega_h$ and $d\sigma_{LT}/d\Omega_h$ give rather large contribution (e.g., for measurements of t- or ϕ_h-dependence), the model independence has to always be tested by comparison with data (or other models) in the collinear regions. This is especially important in the light of recent investigations which demonstrated that in certain cases the MAID 2003 can be imperfect [17].

Examples of RC factor including the exclusive radiative tail contribution are shown on Figs. 4, 5 and 6.

It could be seen in Fig. 4 that the exclusive radiative tail contribution at $z \sim 0.1$ is small or even negligible but rapidly increases with the growing z near SIHL threshold, i.e., when $t \to t_{\min}$. Such behavior appears from the first term in Eq. (14) due to smallness of the

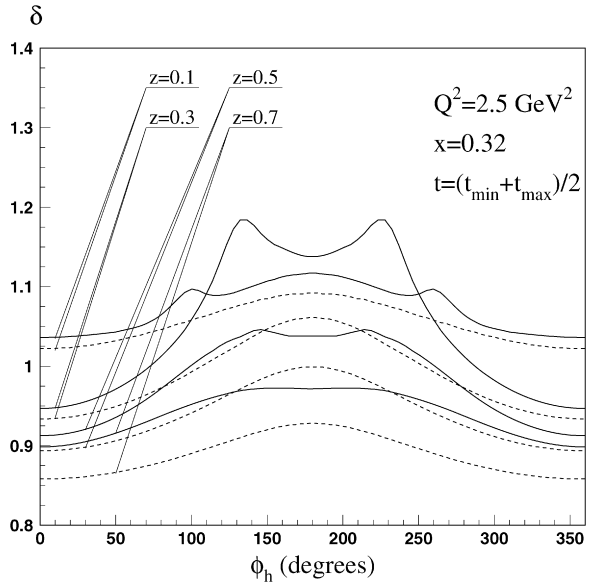

Fig. 5. ϕ_h-dependence of the RC factor (28) for the semi-inclusive π^+ electroproduction at fixed proton for lepton beam energy 6 GeV: solid lines show the total correction, dashed lines represent the correction excluding the exclusive radiative tail calculated in this Letter.

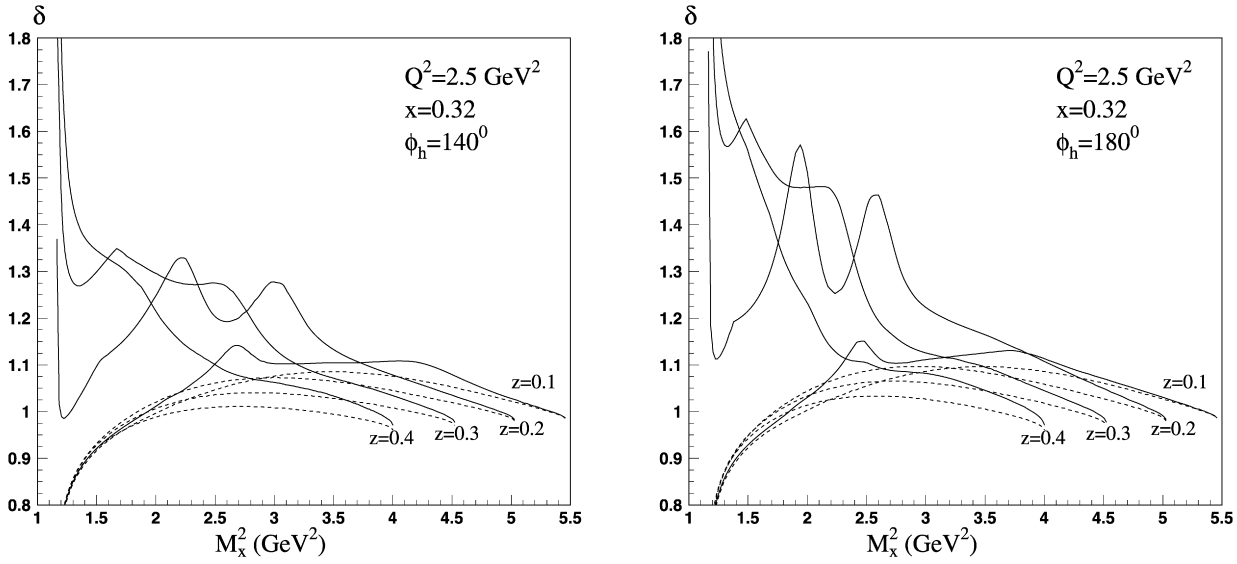

Fig. 6. M_X^2-dependence of the RC factor (28) for the semi-inclusive π^+ electroproduction at fixed proton for lepton beam energy 6 GeV: solid lines show the total correction, dashed lines represent the correction excluding the exclusive radiative tail calculated in this Letter.

denominator in expression for R defined by Eq. (7). In contrast to the elastic radiative tail contribution to inclusive DIS, the minimally allowed value of $\tilde{Q}^2$ (see Eq. (13)) in the integrand of Eq. (13) does not reach the region close to the photon point region $\tilde{Q}^2 \to 0$ where the exclusive cross section increases rapidly. As a result, the so-called t-peak (or Compton peak) often essentially contributing to the cross section of the elastic radiative tail [18,19] does not appear in the considered case, and the main contribution to exclusive radiative tail appears from the collinear region.

The absolute value of the exclusive radiative tail rapidly increases with growing the invariant t (or missing mass of the detected lepton–hadron system). However, the SIHL cross section increases with t much faster making the relative contribution of the exclusive radiative tail small or negligible at large t. Meanwhile, the situation changes to the opposite at small t, i.e., close to the threshold where the exclusive radiative tail exceeds the SIHL cross section (Fig. 4).

Moreover, one can see in Figs. 4 and 5 that the contribution of the exclusive radiative tail can significantly modify the ϕ_h-distributions at middle t distorting usual $A + B\cos\phi_h + C\cos 2\phi_h$ behavior.

Fig. 4 and 5 illustrate that if the at low ϕ_h the exclusive radiative tail contribution to SIHL reaches rather high values near the pion threshold, then with rising ϕ_h up to 180° the correction is rather large for much wider kinematical region. The behavior of the RC factor as a function of missing mass square (27) at $\phi_h = 140°$ and $\phi_h = 180°$ is shown in Fig. 6. From this plot it can be seen that the exclusive radiative tail has a significant contribution in $M_X^2 > (m_u + m_\pi)^2$ already at $z = 0.2$ that shifts to the pion threshold with the growing z. Particularly at $z = 0.2$ and $\phi_h = 140°$ the contribution of the exclusive radiative tail to SIHL exceed 20% in the $M_X^2 \approx 3$ GeV^2 region.

The bump structures in the exclusive tail contribution seen in Figs. 4 and 6 are due to the contribution of nucleon resonances in the MAID parameterization.

Table 1
Relative exclusive radiative tail contribution at different ϕ_h to the observed cross section for the kinematical points of Ref. [20].

	x	Q^2 GeV^2	z	p_t GeV	$\delta-1$			
					$\phi_h=0$	$\phi_h=\pi/4$	$\phi_h=3\pi/4$	$\phi_h=\pi$
$M_X>1.1$ GeV	0.18	1.10	0.61	0.46	0.01558	0.01558	0.01559	0.01561
	0.24	1.30	0.61	0.42	0.02373	0.02374	0.02375	0.02378
	0.31	1.60	0.61	0.41	0.03692	0.03693	0.03695	0.03699
	0.37	2.00	0.61	0.39	0.04650	0.04651	0.04653	0.04656
	0.27	1.46	0.54	0.43	0.01753	0.01753	0.01755	0.01757
	0.27	1.44	0.61	0.43	0.02869	0.02870	0.02872	0.02875
	0.27	1.44	0.69	0.42	0.05847	0.05848	0.05851	0.05857
	0.27	1.43	0.77	0.36	0.1508	0.1508	0.1509	0.1510
$M_X>1.4$ GeV	0.18	1.10	0.58	0.43	0.01286	0.01286	0.01287	0.01289
	0.24	1.40	0.57	0.36	0.01458	0.01459	0.01459	0.01461
	0.31	1.70	0.56	0.32	0.02241	0.02241	0.02242	0.02244
	0.37	2.00	0.56	0.28	0.03573	0.03574	0.03575	0.03577
	0.26	1.44	0.54	0.38	0.01505	0.01481	0.01483	0.01484
	0.25	1.41	0.61	0.34	0.02130	0.02072	0.02073	0.02075
	0.23	1.37	0.69	0.30	0.03438	0.03315	0.03316	0.03318
	0.20	1.26	0.77	0.24	0.05859	0.05602	0.05604	0.05606

In experimental data analyses the five-fold cross sections are estimated in specific bins. There exist several schemes of how radiative correction can be applied to the cross section observed in a certain bin. The simplest and most practical variant is to calculate the RC for the center of the bin, i.e., for means of kinematic variables defining the bin. If the bin is broad over one or several kinematic variables then the Born cross section and the contribution of the exclusive radiative tail can change differently over the bin. In this case the integration over the bin has to be performed with taking into account all experimental cuts which are used by experimentalists to form the bin. The exact procedure to apply the RC to data collected in such bins supposes integration of the cross section of RC over a bin. Since this procedure is computationally extensive, often approximate procedures are used. One possible scheme of such approximate integration is a so-called 'event-by-event' scheme where reweighing the RC factor defined by Eq. (28) is applied for each reconstructed event. Some of experimental cuts used by experimentalists can essentially influence the RC factor for the bin. One often used cut is the cut on missing mass or inelasticity. This cut allows to avoid a contribution of resonances and also it is important for RC calculation. Table 1 presents the results of RC calculation for these two approaches to binning forming (i.e., with and without cutting the resonance region) as used in Ref. [20]. As one can see, applying the cut on missing mass allows to suppress the contribution of the exclusive radiative tail. Note, there are experimental situations where RC including the contribution from the resonance region are of great importance. Examples include the analysis of the measurements of the threshold reactions, e.g., "quark–hadron duality" which is based on a comparison of production in the resonance region with extrapolation of DIS measurements, or reanalysis of older Cornell data from [1] which were collected without any cuts of the threshold region. Therefore, our program includes an option to apply a cut on missing mass squared at the integrand of the cross section of the exclusive radiative tail.

Summarizing, the exclusive radiative tail contribution to complete five-fold differential unpolarized SIHL cross section has been calculated exactly for the first time. Respective FORTRAN code for the numerical estimation is opened for the scientific community. Numerical analysis performed for kinematical conditions of the current experiments at JLab demonstrated that the RC to the SIHL coming from the exclusive radiative tail is high in the regions of small t and close to the threshold while for $\phi_h\sim 180^\circ$ the kinematical region where RC is important is much wider. This contribution significantly modifies ϕ_h-asymmetries of the SIHL cross section. The present approach is quite general and can be extended to other SIHL reactions providing knowledge of the exclusive cross section at the threshold.

The calculated correction to the SIHL due to the radiative tail from exclusive processes is important and its contribution always has to be taken into account in analyses of data in current and future experiments on the SIHL. Currently, this correction is ignored or analyzed in the peaking approximation [10], quality of which can be evaluated only by comparison with exact formulae presented in this Letter. Several sources of systematical uncertainties have to be investigated in the data analyses including (i) the specific choice of the model for the photoproduction cross sections, (ii) quality of peaking approximation, if this approximation is used instead of the exact formulae, and (iii) the choice of specific scheme of radiation correction procedure in a specific bin if it is used instead of exact integration of the radiative tail cross section over the bin.

Acknowledgements

One of us (A.I.) would like to thanks the staff of Istituto Nazionale di Fisica Nucleare (Genova, Italy) for their generous hospitality during his visit.

Appendix A. Structure functions

The following expressions relate the structure functions incoming into (10) to the Born photoabsorption cross sections,

$$\mathcal{H}_1(W^2,Q^2,t)=C\left(\frac{d\sigma_T}{d\Omega_h}-\frac{d\sigma_{TT}}{d\Omega_h}\right),$$

$$\mathcal{H}_2(W^2,Q^2,t)=\frac{2C}{\lambda_q}\left[2Q^2\left(\frac{d\sigma_T}{d\Omega_h}-\frac{d\sigma_{TT}}{d\Omega_h}+\frac{d\sigma_L}{d\Omega_h}\right)-2TQ\,\frac{d\sigma_{LT}}{d\Omega_h}+T^2\frac{d\sigma_{TT}}{d\Omega_h}\right],$$

$$\mathcal{H}_3(W^2,Q^2,t)=\frac{2C\lambda_q}{\lambda_l}\frac{d\sigma_{TT}}{d\Omega_h},$$

$$\mathcal{H}_4(W^2, Q^2, t) = \frac{2C}{\sqrt{\lambda_l}}\left(T\frac{d\sigma_{TT}}{d\Omega_h} - Q\frac{d\sigma_{LT}}{d\Omega_h}\right), \tag{A.1}$$

in such a way, that five-fold differential cross section for exclusive leptoproduction has a standard form [15,21]

$$\frac{d\sigma}{dE_2\, d\Omega_2\, d\Omega_h} = \Gamma\left[\frac{d\sigma_T}{d\Omega_h} + \varepsilon\frac{d\sigma_L}{d\Omega_h} + \sqrt{2\varepsilon(1+\varepsilon)}\frac{d\sigma_{LT}}{d\Omega_h}\cos\phi_h + \varepsilon\frac{d\sigma_{TT}}{d\Omega_h}\cos 2\phi_h\right],$$
$$\Gamma = \frac{\alpha}{2\pi^2}\frac{E_2}{E_1}\frac{\kappa_\gamma}{Q^2}\frac{1}{1-\varepsilon}, \quad \kappa_\gamma = \frac{W^2-M^2}{M^2}, \quad \varepsilon = \left(1 + \frac{\lambda_q}{2(SX - M^2Q^2)}\right)^{-1}. \tag{A.2}$$

Here $E_1 = S/2M$ ($E_2 = X/2M$) is the initial (final) lepton energy in the target rest frame system, $d\Omega_2$ ($d\Omega_h$) is a element of solid angle of scattering lepton (detected hadron) in the target rest frame (c.m. system of the virtual photon and target),

$$C = \frac{16\pi(W^2-M^2)W^2}{\alpha\sqrt{(W^2+m_h^2-m_u^2)^2 - 4m_h^2W^2}}, \qquad T = \frac{S_x(t_q - 2zQ^2)}{\sqrt{\lambda_l}},$$
$$\lambda_l = zS_x^2(zQ^2 - t_q) - M^2t_q^2 - m_h^2\lambda_q, \quad t_q = t + Q^2 - m_h^2 \tag{A.3}$$

and $Q = \sqrt{Q^2}$.

Appendix B. Some kinematic quantities

The scalar products of p_h in $V_{1,2}$ and μ (see Eq. (4)) are expressed via coefficients a^1, a^2, b, a^k and b^k:

$$2Ma^1 = SE_h - \left(SS_x + 2M^2Q^2\right)p_l\lambda_q^{-1/2}, \qquad 2Ma^2 = XE_h - \left(XS_x - 2M^2Q^2\right)p_l\lambda_q^{-1/2}, \qquad b = -p_t\sqrt{\lambda/\lambda_q},$$
$$2Ma^k = E_h - p_l\left(S_x - 2M^2\tau\right)\lambda_q^{-1/2}, \qquad b^k = -Mp_t\sqrt{\lambda_\tau/\lambda_q}, \tag{B.1}$$

where

$$\lambda_\tau = (\tau - \tau_{\min})(\tau_{\max} - \tau), \qquad \lambda = SXQ^2 - M^2Q^4 - m^2\lambda_q. \tag{B.2}$$

Quantities θ_{ij} (see Eq. (14)) have the following form:

$$\theta_{12} = 4F_{IR}\tau,$$
$$\theta_{13} = -4 - 2F_d\tau^2,$$
$$2\theta_{22} = F_{1+}S_xS_p - F_d\tau S_p^2 + 2m^2F_{2-}S_p + 2F_{IR}\left(S_x - 2M^2\tau\right),$$
$$2\theta_{23} = F_d\left(4m^2 + \tau\left(2M^2\tau - S_x\right)\right) - F_{1+}S_p + 4M^2,$$
$$\theta_{32} = 2\left(F_{IR}\left(\mu V_- - m_h^2\tau\right) + m^2F_{2-}\mu V_+ + F_{1+}V_+V_- - F_d\tau V_+^2\right),$$
$$\theta_{33} = F_d\left(2m^2\mu^2 + \tau\left(m_h^2\tau - \mu V_-\right)\right) - 2F_{1+}\mu V_+ + 2m_h^2,$$
$$\theta_{42} = -2F_d\tau V_+S_p + F_{1+}(S_xV_+ + S_pV_-) + m^2F_{2-}(\mu S_p + 2V_+) + F_{IR}\left((\mu - 2\tau z)S_x + 2V_-\right),$$
$$2\theta_{43} = F_d\left(8\mu m^2 + \tau\left((2\tau z - \mu)S_x - 2V_-\right)\right) - F_{1+}(\mu S_p + 2V_+) + 4S_xz. \tag{B.3}$$

Here $V_\pm = (V_1 \pm V_2)/2$, $F_{IR} = m^2F_{2+} - (Q^2 + 2m^2)F_d$, and

$$F_d = \frac{1}{z_1z_2}, \qquad F_{1+} = \frac{1}{z_1} + \frac{1}{z_2}, \qquad F_{2-} = \frac{1}{z_2^2} - \frac{1}{z_1^2}, \qquad F_{2+} = \frac{1}{z_2^2} + \frac{1}{z_1^2}. \tag{B.4}$$

The variable $z_{1,2}$ can be expressed as in Ref. [6]

$$z_1 = \frac{2kk_1}{R} = \frac{1}{\lambda_q}\left[Q^2S_p + \tau\left(SS_x + 2M^2Q^2\right) - 2M\cos\phi_k\sqrt{\lambda_\tau\lambda}\right],$$
$$z_2 = \frac{2kk_2}{R} = \frac{1}{\lambda_q}\left[Q^2S_p + \tau\left(XS_x - 2M^2Q^2\right) - 2M\cos\phi_k\sqrt{\lambda_\tau\lambda}\right]. \tag{B.5}$$

References

[1] C.J. Bebek, et al., Phys. Rev. D 15 (1977) 3085;
C.J. Bebek, et al., Phys. Rev. D 16 (1977) 1986.
[2] L.W. Mo, Y.S. Tsai, Rev. Mod. Phys. 41 (1969) 205.
[3] A. Airapetian, et al., Eur. Phys. J. C 21 (2001) 599.
[4] M. Arneodo, et al., Z. Phys. C 34 (1987) 277.
[5] A.V. Soroko, N.M. Shumeiko, Yad. Fiz. 49 (1989) 1348, Sov. J. Nucl. Phys. 53 (1991) 628.
[6] I. Akushevich, N. Shumeiko, A. Soroko, Eur. Phys. J. C 10 (1999) 681.
[7] D.Yu. Bardin, N.M. Shumeiko, Nucl. Phys. B 127 (1977) 242.
[8] I. Akushevich, A. Ilyichev, N. Shumeiko, A. Soroko, A. Tolkachev, Comput. Phys. Commun. 104 (1997) 201.
[9] I.V. Akushevich, N.M. Shumeiko, J. Phys. G 20 (1994) 513.

[10] T. Navasardyan, et al., Phys. Rev. Lett. 98 (2007) 022001;
T. Navasardyan, PhD thesis, 2006 (Yerevan).
[11] I. Akushevich, Eur. Phys. J. C 8 (1999) 457.
[12] A. Afanasev, I. Akushevich, V. Burkert, K. Joo, Phys. Rev. D 66 (2002) 074004.
[13] L. Trentadue, G. Veneziano, Phys. Lett. B 323 (1994) 201.
[14] J.D. Bjorken, S.D. Drell, Relativistic Quantum Fields, McGraw–Hill, New York, 1965.
[15] D. Drechsel, S.S. Kamalov, L. Tiator, Nucl. Phys. A 645 (1999) 145;
The code is available on http://www.kph.uni-mainz.de/MAID/maid2003/.
[16] A. Browman, et al., Phys. Rev. Lett. 35 (1975) 1313.
[17] K. Park, et al., Phys. Rev. C 77 (2008) 015208.
[18] I.V. Akushevich, T.V. Kukhto, F. Pacheco, J. Phys. G 18 (1992) 1737.
[19] I.V. Akushevich, A.N. Ilyichev, N.M. Shumeiko, Phys. At. Nucl. 61 (1998) 2154, Yad. Fiz. 61 (1998) 2268.
[20] H. Avakian, et al., CLAS Collaboration, Phys. Rev. D 69 (2004) 112004.
[21] D. Drechsel, L. Tiator, J. Phys. G 18 (1992) 449.